GLOBAL SCHEME FOR ITERATIVE MOJETTE RECONSTRUCTIONS

Benoit Recur[1], *Henri Der Sarkissian*[2,3], *Myriam Servieres*[4]

[1]Dept. Applied Math., RSPE, Australian National University, Australia
[2]LUNAM Université, Université de Nantes, IRCCyN UMR CNRS 6597,
Polytech Nantes, rue Christian Pauc BP 50609, 44306 Nantes, France
[3]Keosys - 1, impasse Augustin Fresnel - BP 60227 - 44815 Saint-herblain cedex - FRANCE
[4]LUNAM Université, Ecole Centrale de Nantes, CERMA UMR CNRS 1563,
Rue de la Noë, BP 92101, 44321 Nantes Cedex 3, France

ABSTRACT

In this paper, we develop a global iterative algorithm for tomographic reconstructions from Mojette projections. Since Spline-Mojette projections are obtained by convolving Dirac-Mojette values with a specific uniform projection kernel, we decorrelate iterative reconstructions from projection model and provide a global scheme available for all Mojette models. We refer iterative algorithms to their Radon based counterparts and propose a comparative study from several Mojette acquisitions.

Index Terms— Discrete geometry, Mojette transform, Tomography, Iterative techniques.

1. INTRODUCTION

In the field of medical or industrial tomography, iterative algorithms such that Simultaneous Algebraic Reconstruction Technique (SART) [1, 2] or Ordered Subset Expectation Maximization (OSEM) [3, 4] are widely used to reconstruct a volume from its projections. These methods are particularly powerful to reconstruct from a few number of noisy projections, with high quality and accuracy compared to the direct Filtered Backprojection (FBP) [5].

Apart from standard Radon based tomography [5], the Mojette transform has been developed during the two last decades as a discrete version the Radon transform. This transform is exact in the sense that the acquired image can be reconstructed exactly using Corner Based Inversion (CBI) from noise-free projections [6]. This property has made the Mojette transform very suitable in many application fields such that encryption, watermarking, cloud computing and distributed storage [7, 8, 9, 10].

More recently, several Radon-to-Mojette mappings have been investigated. They allow one to reconstruct from real tomographic data using Mojette theory with competitive quality results compared to standard algorithms [11, 12]. These new insights were particularly motivated by the fact that rigid transforms (reorientations, upscalings) in Mojette space [13] can be performed without interpolations. Then, contrary to continuous based transforms, rigid transforms in Mojette spaces consist of an exact and reversible processing which does not degradate reoriented reconstructed volume quality.

However, apart from the exact CBI algorithm, only few reconstruction methods have been proposed to recover an image from noisy Mojette projections. We can denote for example the Noise Robust CBI algorithm [14] or the FBP-Mojette [15]. Even if few iterative algorithms have also been proposed, such that SART-Mojette, they refer to a specific iterative model, available for a specific Mojette acquisition, and the litterature remains scattered [14].

Thus in this paper, we investigate the algebraic as well as the Bayesian approaches in order to provide an iterative scheme for Mojette reconstructions. After introducing Radon based iterative theory (section 2), we detail Mojette transform definitions (section 3). We develop Mojette based iterative techniques in section 4, allowing us to define ART and EM algorithms for Dirac-Mojette and Spline-Mojette [16] domains. A comparison of images reconstructed from Mojette projections is finally discussed in section 5.

2. RADON BASED ITERATIVE TECHNIQUES

Usual tomographic devices are based on Radon's theorem [5] to reconstruct the volume of an object from a projection set acquired from the exterior of the object. The Radon transform $\mathcal{R}$ describes the projection line acquisition. It maps a function $f(x, y)$ into its projections along angles θ and positions ρ as follows :

$$\mathcal{R}_\theta(\rho) = \iint_{-\infty}^{\infty} f(x,y)\delta(\rho - x\cos\theta - y\sin\theta)dxdy \quad (1)$$

where θ and ρ are respectively the angular and radial coordinates of the projection line (θ, ρ) and $\delta(\cdot)$ is the Dirac impulse. As an illustration, the Shepp-Logan phantom [17] and

Thanks to KEOSYS SAS, Quanticardi project from region Pays de la Loire and Australian National Low Emissions Coal for funding this work.

its Radon transform (called sinogram) performed using 180 angles uniformly distributed between 0 and π, with 512 samples per projection are depicted Fig. 1.

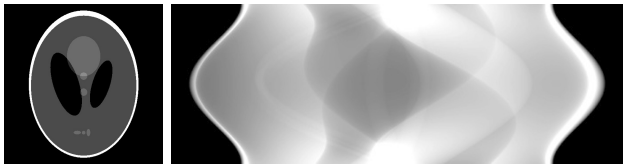

(a) (b)

Fig. 1. (a) Shepp-Logan phantom represented in an image sized 512×512. (b) Acquired 180 projections sinogram of 512 samples.

Tomographic reconstruction consists of inverting the Radon transform, ie. recovering $f(x, y)$ from a given projection set R. A wide kind of algorithms such as FBP or iterative techniques are now well established to compute such an image from its projections [1, 2, 3].

2.1. Simultaneous Algebraic Reconstruction Technique

The simultaneous algebraic reconstruction technique [1, 2] (SART) approaches the solution of the linear equation system $I = A^{-1}R$, where I is the image, R is the sinogram and A is a pixel-to-projection weight-matrix, using an iterative processing following $k \in [0 \cdots N_{iter}[$, where N_{iter} is the number of iterations. Each sub-iteration s, $0 \leq s < N_\theta$, updates each pixel of the image $I^{k,s}$ by comparing the measured projection R_{θ_s} with $R^k_{\theta_s}$ (computed from $I^{k,s-1}$) as follows :

$$I^{k,s}(i,j) = I^{k,s-1}(i,j) + \frac{\sum_{\rho=0}^{N_\rho - 1} A_{(\theta,\rho),(i,j)} \left[\frac{R_{\theta_s}(\rho) - R^k_{\theta_s}(\rho)}{D_{\theta_s}(\rho)} \right]}{\sum_{\rho=0}^{N_\rho - 1} A_{(\theta,\rho),(i,j)}} \tag{2}$$

where N_θ is the projection number, N_ρ is the sample number on each projection, $D_\theta(\rho) = \sum_{i=0}^{W-1} \sum_{j=0}^{H-1} A_{(\theta,\rho),(i,j)}$ corresponds to the norm of segment (θ, ρ) crossing the image, $R^k_{\theta_s}(\rho)$ is computed from image at previous iteration using Eq. (1) and $(W \times H)$ is the image size. A super-iteration k is completed when all the projections have been used. Iterations in k are performed until the convergence of the solution.

2.2. Expectation Maximization Techniques

Expectation Maximization [3, 4] relies on a wide range of iterative algorithms based on Bayesian theory. An update step of the algorithm is performed as follows :

$$I(i,j)^{k+1} = I(i,j)^k \frac{\sum_{\theta=0}^{N_\theta - 1} \sum_{\rho=0}^{N_\rho - 1} A_{(\theta,\rho),(i,j)} \frac{R_\theta(\rho)}{R^k_\theta(\rho)}}{U(i,j) + \sum_{\theta=0}^{N_\theta - 1} \sum_{\rho=0}^{N_\rho - 1} A_{(\theta,\rho),(i,j)}} \tag{3}$$

where $U(i, j)$ is a regularization term taking into account the neighborhood behaviour of updated pixel as defined in [18, 19, 20].

2.3. Iterative Algorithm scheme

Globally, an iterative algorithm (cf. Fig. 2) consists of iterating the following steps : 1) select a projection or a set s of projection angles ; 2) compute corresponding forward projections from the image at previous iteration ; 3) compute the projection errors by an additive or multiplicative comparison between each measured and computed projection ; 4) update the image by retroprojecting the errors and taking into account regularizations (backprojection).

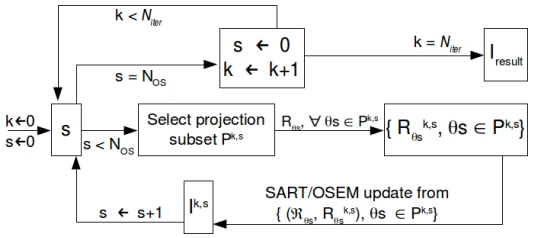

Fig. 2. Global iterative reconstruction algorithm.

Iterative algorithms are powerful to deal with deblurring from detector response function. Indeed, an acquisition detector response can be modeled as a convolution filter applied on the forward projection. It consists of redefining the overall acquisition function Eq. (1) with $f'(x, y) = M(x, y) \star f(x, y)$ or $R'_\theta(\rho) = M_p(\rho) \star R_\theta(\rho)$, where $M(x, y)$ (*resp.* $M_p(\rho)$) denotes an image (*resp.* a projection) filter and $\star$ is the convolution operator. Thus such an algorithm corrects for acquisition defects using direct response model in forward process, avoiding deconvolutions (inverse model) needed when one uses analytic reconstruction (FBP).

3. MOJETTE TRANSFORM

The Dirac-Mojette transform [6, 16] is a discrete version of the Radon transform using angles defined by $\tan\theta = \frac{q}{p}$ such that $(p, q) \in \mathbb{Z}^2$ are co-prime and correspond to the number of pixel displacement horizontally and vertically. A projection value (called a bin) $M_{p,q}(b)$ on a projection (p, q) is the sum of pixels centered on the line $b = pj - qi$:

$$M_{p,q}(b) = \sum_{i=0}^{W-1} \sum_{j=0}^{H-1} I(i,j) \Delta(b - pj + qi) \tag{4}$$

where I is a 2D orthonormal support lattice sized $W \times H$ and $I(i, j)$ is the pixel value. (p, q)-projection size is $N_\rho(p, q) = (W - 1)|q| + (H - 1)|p| + 1$.

The Spline-Mojette transform extends the Dirac-Mojette transform to consider each bin as a weighted sum of pixels along a discrete line [16]. This model is closer to the

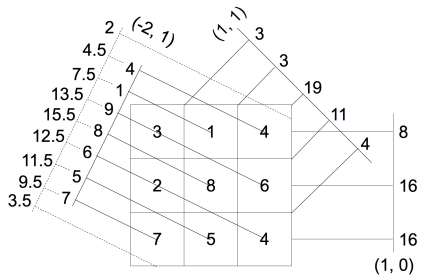

Fig. 3. Dirac-Mojette projections $(-2,1)$, $(1,1)$ and $(1,0)$ computed from a 3×3 pixel image : each pixel is projected exactly in one bin of each projection. Spline-Mojette $(-2,1)$-projection values are also provided : all pixels are uniformly projected into several bins according to the Spline kernel of the discrete projection.

continuous beam propagation [11] encountered in Radon acquisitions. Spline-Mojette bins $M^S_{p,q}(b)$ can be computed by applying the Spline kernel $S_{p,q}(x)$ as a convolution filter on Dirac-Mojette bins or by a direct image acquisition using $S_{p,q}(x)$ as pixel-weight function :

$$\begin{aligned} M^S_{p,q}(b) &= \sum_{i=0}^{W-1}\sum_{j=0}^{H-1} I(i,j) S_{p,q}(b-pj+qi) \\ &= \sum_{b' \in (p,q)} M_{p,q}(b) S_{p,q}(b-b') \end{aligned} \tag{5}$$

where :

$$S_{p,q}(x) = \begin{cases} 1 \text{ if } 2x \leq ||p|-|q|| \\ \dfrac{-2x+|p|+|q|}{2\min\{|p|,|q|\}} \text{ if } ||p|-|q|| < 2x < |p|+|q| \\ 0 \text{ elsewhere} \end{cases} \tag{6}$$

An example of Dirac-Mojette and Spline-Mojette projections acquired from a 3×3 pixel image is given on Fig. 3.

4. ITERATIVE MOJETTE RECONSTRUCTIONS

4.1. Algebraic Mojette Reconstruction

Eq. (2) can be written as follows to obtain a Dirac-Mojette algebraic update step :

$$I^{k,s}(i,j) = I^{k,s-1}(i,j) + \frac{\displaystyle\sum_{b\in(p,q)} \Delta(x) \left[\frac{M_{p,q}(b) - M^{k,s}_{p,q}(b)}{\displaystyle\sum_{i'=0}^{W-1}\sum_{j'=0}^{H-1} \Delta(b-j'p+i'q)} \right]}{\displaystyle\sum_{b\in(p,q)} \Delta(x)} \tag{7}$$

where $x = b - pj + qi$. Since Dirac pulse implies $\Delta(x) = 1$ when $b = pj - qi$ and 0 otherwise, Eq. (7) is simplified by :

$$I^{k,s}(i,j) = I^{k,s-1}(i,j) + \left[\frac{M_{p,q}(b) - M^{k,s}_{p,q}(b)}{||b_{p,q}||} \right] \tag{8}$$

where $b = pj - qi$, $M_{p,q}(b)$ is the original Mojette acquisition, $M^{k,s}_{p,q}(b)$ is computed from image $I^{k,s-1}$ using Eq. (4) and $||b_{p,q}|| = \displaystyle\sum_{i=0}^{W-1}\sum_{j=0}^{H-1} \Delta(b-pj+qi)$ is the number of pixels crossed by bin b on projection (p,q).

This simplication can not be done with Spline-Mojette projections since several values of $S_{p,q}(b)$ differ from 0 :

$$I^{k,s}(i,j) = I^{k,s-1}(i,j) + \frac{\displaystyle\sum_{b\in(p,q)} S_{p,q}(x) \left[\frac{M^S_{p,q}(b) - M^{S,k,s}_{p,q}(b)}{||b^S_{p,q}||} \right]}{\displaystyle\sum_{b\in(p,q)} S_{p,q}(x)} \tag{9}$$

where $M^S_{p,q}(b)$ is the original Spline-Mojette acquisition, $M^{S,k,s}_{p,q}(b)$ is computed from image $I^{k,s-1}$ using Eq. (5) and $||b^S_{p,q}|| = \displaystyle\sum_{i'=0}^{W-1}\sum_{j'=0}^{H-1} S_{p,q}(b-j'p+i'q)$ is the discrete distance crossed by bin b in the image.

Spline kernel S is uniform when it is applied as a pixel-weight during acquisition or as a convolution filter on Dirac-Mojette bins. Then, as explained in section 2.3, it can be viewed as a blurring effect to correct for during the iterations. In that case, forward and back-projections remain Dirac based, resulting to the following update step :

$$I^{k,s}(i,j) = I^{k,s-1}(i,j) + \left[\frac{M^S_{p,q}(b) - M^{k,s}_{p,q}(b) \star S}{||b_{p,q}||} \right] \tag{10}$$

4.2. Expectation Maximization Mojette

Similar approach can be followed to obtain a Mojette Expectation-Maximization. Let P_S be a subset of projections in P and $||P_S||$ be the number of projections in P_S, a Spline-Mojette version of Eq. (3) (considering simplifications made above) can be :

$$I^{k,s}(i,j) = I^{k,s-1}(i,j) \frac{\displaystyle\sum_{(p,q)\in P_S} \left[\frac{M^S_{p,q}(b)}{M^{k,s}_{p,q}(b) \star S} \right]}{||P_S||} \tag{11}$$

where the regularization term in Eq. (3) is ignored. $P_S = P$ relies on EM [3] whereas $P_S \neq P$ leads to OSEM [4].

4.3. Global Iterative Mojette Algorithm

The overall scheme of an iterative reconstruction from Mojette projections remains the same than on Fig. 2. However one can remark that computations are simplified due to the uniform one-to-one mapping between pixels and bins. This property allows to consider the Spline-kernel S (and any other uniform pixel-to-projection weighting functions) as a convolution filter to correct for instead of a specific Mojette forward and backward modelling. It results that iterative Mojette reconstructions are projection-kernel invariant.

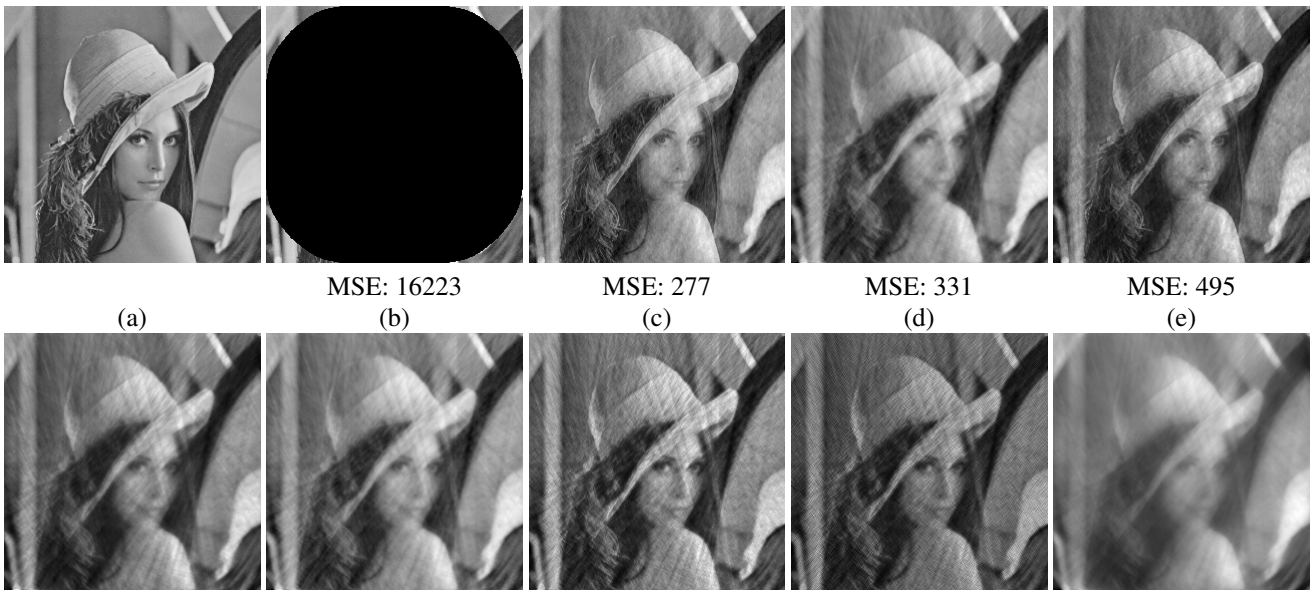

Fig. 4. (a) Original 256×256 image. (b) Incomplete CBI reconstruction F_6 projection set. Reconstructions using 5 iterations and 4 sub-sets obtained by : (c) SART-Mojette from Mojette bins ; (d) SART-Mojette from Spline-Mojettes bins ; (e) OSEM-Mojette from Mojette bins ; (f) OSEM-Mojette from Spline-Mojette bins. OSEM-Mojette reconstructions from Spline-Mojette bins using : (g) 5 iterations and (h) 10 iterations with projection by projection update ; (i) 10 iterations and 1 subset.

5. RECONSTRUCTION EXAMPLES

The original image is a 256×256 view of the well-known Lenna image (cf. Fig. 4(a)). This image is acquired using the projection set F_6 given by the Farey-Haros series of order 6 and symmetries [21]. This projection set contains 48 projections, which is not enough to obtain a complete reconstruction using CBI from noise-free projections (cf. Fig. 4(b)). Reconstructions from Dirac-Mojette and Spline-Mojette bins using Algebraic and EM methods are given in Fig. 4(c-f). We have used 4 subsets of 12 projections and 5 iterations. MSE results are obtained by comparing reconstructed images with the original. They highlight better quality results from Dirac projections whatever the reconstruction.

As a comparison, SART reconstruction on Fig. 4(g) is obtained by update step Eq. (9) whereas SART reconstruction on Fig. 4(d) was obtained by Eq. (10). Similarity between both results confirm that Spline kernel can be considered as a blurring filter to correct for instead of a specific forward/backward model. Finally, image Fig. 4(h) (*resp.* Fig. 4(i)) is obtained by OSEM-Mojette using 5 (*resp.* 10) iterations and a projection-by-projection update. Fig. 4(j) is obtained by 10 iterations with 1 subset. These results confirm that convergence speed and divergence depend both on the iteration and ordered-subset numbers ; which relies on similar well-known results of usual tomography.

6. CONCLUSION

Iterative techniques, based on algebraic or Bayesian theory, are widely used in standard tomography. We have demonstrated in this paper that they can be adapted to the Mojette transform. Moreover, their overall computation is simplified by the uniform mapping between pixels and bins. Indeed, uniform weight coefficients in the forward projection (such that Spline-Mojette) can be viewed as a blurring convolution filter to correct for from Dirac-Mojette bins. This property allows to define a global scheme where forward and back-projections are always based on Dirac modelling. Thus scheme is used to provide any algebraic or stochastic algorithm, whatever the kind of measured Mojette projections.

However in that study, we have neglected the regularization term used to add an *a priori* on the reconstructed image. Such regularisation often consists of penalizing pixel update according to the behaviour of pixel neighborhood. In Mojette geometry, neighborhood definition is quite different since acquisition is composed of pixels which are not adjacent. Then our future works will focus on the investigation of regularization terms for Mojette iterative reconstructions, taking into account the specific properties of such discrete neighborhoods. They will be used for reconstructing images from Radon-to-Mojette interpolated projections [11, 12].

7. REFERENCES

[1] R. Gordon, R. Bender, and G. T. Herman, "Algebraic Reconstruction Techniques (ART) for Three-dimensional Electron Microscopy and X-ray Photography," *Journal of Theoretical Biology*, vol. 29, pp. 471 – 481, 1970.

[2] A. H. Andersen and A. C. Kak, "Simultaneous algebraic reconstruction technique (sart): a superior implementation of the art algorithm," *Ultrasonic imaging*, vol. 6, no. 1, pp. 81 – 94, 1984.

[3] L. A. Shepp and Y. Vardi, "Maximum likelihood reconstruction for emission tomography," *IEEE Transactions on Medical Imaging*, vol. 1, no. 2, pp. 113 – 122, october 1982.

[4] H. M. Hudson and R. S. Larkin, "Accelerated image reconstruction using ordered subsets of projection data," *IEEE Transactions on Medical Imaging*, vol. 13, no. 4, pp. 601 – 609, december 1994.

[5] J. Radon, "Uber die Bestimmung von Funktionen durch ihre Integralwerte langs gewisser Mannigfaltigkeiten.," *Ber. Ver. Sachs. Akad. Wiss. Leipzig, Math-Phys. Kl*, vol. 69, pp. 262–277, April 1917, In German. An english translation can be found in S. R. Deans : The Radon Transform and Some of Its Applications.

[6] J.-P. Guédon, Ed., *The Mojette Transform : Theory and Applications.*, ISTE-Wiley, 2009.

[7] F. Autrusseau and Jp. Guedon, "Image watermarking for copyright protection and data hiding via the mojette transform," in *Electronic Imaging 2002*. International Society for Optics and Photonics, 2002, pp. 378–386.

[8] M. Babel, B. Parrein, O. Deforges, N. Normand, Jp. Guedon, and J. Ronsin, "Secured and progressive transmission of compressed images on the internet: application to telemedicine," in *Electronic Imaging 2005*. International Society for Optics and Photonics, 2005, pp. 126–136.

[9] Jp. Guédon, B. Parrein, and N. Normand, "Internet distributed image information system," *Integrated Computer-Aided Engineering*, vol. 8, no. 3, pp. 205–214, 2001.

[10] P. Verbert, V. Ricordel, Jp. Guédon, et al., "Analysis of mojette transform projections for an efficient coding," in *Workshop on Image Analysis for Multimedia Interactive Services (WIAMIS)*, 2004.

[11] B. Recur, H. Der Sarkissian, M. Servières, N. Normand, and Jp. Guédon, "Validation of mojette reconstructions from radon acquisitions," *IEEE International Conference in Image Processing (ICIP)*, pp. 1041–1045, September 2013.

[12] H. Der Sarkissian, B. Recur, Jp. Guédon, P. Bléry, and Y. Amouriq, "Mojette tomographic reconstruction for micro CT: a bone and vessels quality evaluation," *SPIE Medical Imaging, San Diego*, vol. 9038, no. 37, February 2014.

[13] H. Der Sarkissian, B. Recur, N. Normand, and Jp Guédon, "Rotations in the mojette space," *IEEE International Conference in Image Processing (ICIP)*, pp. 1187–1191, September 2013.

[14] B. Recur, P. Desbarats, and J.-P. Domenger, "Noise robust mojette reconstructions for missing wedge effect attenuation.," *JMPT*, vol. 1, no. 4, pp. 209–227, 2010.

[15] M. Servières, N. Normand, P. Subirats, and Jp. Guédon, "Some links between continuous and discrete Radon transform," in *Society of Photo-Optical Instrumentation Engineers (SPIE) Conference Series*, J. M. Fitzpatrick and M. Sonka, Eds., May 2004, vol. 5370 of *Society of Photo-Optical Instrumentation Engineers (SPIE) Conference Series*, pp. 1961–1971.

[16] J.-P. Guédon and N. Normand, "Spline Mojette Transform : Applications in Tomography and Communications," *EUSIPCO*, vol. 3, pp. 271–274, 2002.

[17] L. Shepp and B. Logan, "The Fourier Reconstruction of a Head Section," *IEEE Transactions in Nuclear Science*, vol. 21, no. 2, pp. 21 – 43, 1974.

[18] S. Geman and D. McClure, "Statistical methods for tomographic image reconstruction," *Bull. Int. Stat. Inst.*, vol. LII-4, pp. 5 – 21, 1987.

[19] T. Hebert and R. Leahy, "A generalized em algorithm for 3-d bayesian reconstruction from poisson data using gibbs priors," *IEEE Transactions on Medical Imaging*, vol. 8, no. 2, pp. 194 – 202, june 1990.

[20] S. Saquib, C. Bouman, and K. Sauer, "ML parameter estimation for markov random fields with applications to bayesian tomography," *IEEE Transactions on Image Processing*, vol. 7, no. 7, pp. 1029 – 1044, july 1998.

[21] M. Servières, N. Normand, Jp. Guédon, and Y. Bizais, "The mojette transform: Discrete angles for tomography," *Electronic Notes in Discrete Mathematics*, vol. 20, pp. 587 – 606, 2005.